SER-Based Connectivity of Fading Ad-Hoc Networks

Homayoun Yousefi'zadeh Hamid Jafarkhani Javad Kazemitabar
Department of EECS
University of California, Irvine

[hyousefi,hamidj,skazemit]@uci.edu

***Abstract*— Received signal strength has been widely used as the main criterion of connectivity between wireless nodes. We investigate the connectivity of fading wireless ad-hoc networks with a novel connectivity metric. Our metric of connectivity considers realistic effects of the characteristics of the utilized wireless nodes such as modulation and symbol error rate. We assume a pair of nodes are connected if the bi-directional symbol error rate on their direct connecting link is below a given threshold. Our treatment of the problem relies on a probabilistic approach describing the quantities of interest in the form of random variables. Our simulation results over sample ad-hoc topologies support the fact that depending on the characteristics of the wireless nodes, different connectivity results may be observed for the same signal strength.**

***Index Terms*— Wireless Ad-Hoc Networks, Connectivity, Rayleigh Fading Channel, Modulation, Symbol Error Rate.**

I. Introduction

Wireless ad-hoc networks are a special class of adaptively self-organizing wireless networks in which any mobile node can transmit, receive, or relay signals. Eliminating the need for any fixed infrastructure has made the deployment of wireless ad-hoc networks attractive from an operational and economical standpoint. However, strong tendency for the deployment of ad-hoc networks has encountered major challenges due to sometimes conflicting time-varying fading channel, connectivity, capacity, and power issues.

Investigating the connectivity of radio networks and subsequently wireless ad-hoc networks goes back to four decades ago. In his pioneering work, Gilbert [7] studied the connectivity of infinite random networks relying on the so-called geometric disk model and percolation theory [12], [8]. In the geometric disk model, a random topology network is represented by a disk graph in which two nodes are considered directly connected if their distance is smaller than a given transmission radius. Percolation theory revolves around finding conditions under which a node belongs to an unbounded cluster of connected nodes. The work of Gilbert showed that there exists a minimum number of nodes within a transmission range above which a random graph is almost surely connected. It also triggered a rich set of follow on studies in applying percolation theory concepts and the geometric disk model to the connectivity of random networks.

This work was supported in part by the U. S. Army Research Office under the Multi-University Research Initiative (MURI) grant number W911NF-04-1-0224.

Recently, the connectivity subject has received much attention due to the deployment of wireless ad-hoc networks. Some of the recent studies about the connectivity of infinite random networks relying on the geometric disk model include the work of Booth et al. [3], Philips et al. [**?**], and Quintanilla et al. [14]. In addition, a survey of the literature reveals a large number of articles in the context of connectivity of ad-hoc networks with a finite number of mobile nodes. Some of the related articles in this area are summarized below. Cheng et al. [4] introduced a recursion for calculating the average number of hops between two connected nodes. Gupta et al. [10] proved that a large number of nodes in an ad-hoc network are almost surely connected under some mild assumption on the transmission radius. Santi et al. [15] calculated the probability that a finite number of nodes on a given interval are connected. Bettstetter [2] looked at k-connectivity characteristics in a 2-D space under fixed power assumptions. Doussi et al. [5] investigated percolation properties of the random graphs associated with Poisson Boolean model as a mean of connectivity for wireless ad-hoc networks.

Although an attractive abstract model for studying the connectivity, the geometric disk model is far from the reality of wireless networks. Wireless networks are subject to temporally correlated loss due to the time-varying fading effects. Further considering the mobility of the nodes, wireless links are subject to the Doppler spread. The main disadvantages of the disk model have to do with not considering the effects of attenuation, interference, and noise in wireless networks subject to time-varying fading effects. Some of the recent literature articles have, hence, introduced other connectivity metrics that consider the effects of power, interference, and noise. While increasing transmission power in high density areas can lead to reducing the received signal strength between adjacent nodes due to undesired effects of interfer-

ence and noise, reducing transmission power in low density areas can lead to disconnecting adjacent nodes due to low signal strength. In order to capture the effects of interference and power, Gupta et al. [11] proposed the use of signal-to-interference-noise-ratio ($SINR$) as the metric of connectivity in wireless ad-hoc networks. According to $SINR$ metric, two nodes in a random topology are directly connected if their minimum $SINR$ is greater than a given threshold. Relying on the $SINR$ metric and considering a finite random topology network with known per node transmission rates, the authors introduced the attainable per node throughput toward a randomly chosen destination. Baccelli et al. [1] utilized the $SINR$ model under Poisson assumptions in the context of infinite CDMA networks. Relying on the same $SINR$ connectivity metric, Dousse et al. [6] showed that if both node density per unit area and $SINR$ are sufficiently high, the resulting infinite graph of an ad-hoc network is almost surely connected. Grossglauser et al. [9] argued that the capacity of an ad-hoc network can be significantly improved by making use of mobility and multi-user diversity. Interestingly, connectivity in random networks represented by graphs of mixed short and long edges can also be related to small world networks [17].

While $SINR$ is a more realistic metric of connectivity compared to the geometric disk model for wireless ad-hoc networks, it is still not fully capable of capturing the physical connectivity phenomenon. In reality, a pair of nodes are connected if a sequence of transmitted symbols from one can be received at another. In addition, the considerations of time and frequency can also affect the interpretation of connectivity. Hence, utilizing Symbol Error Rates (SER) can better describe the connectivity phenomenon. Symbol error rates and capacity are affected by a variety of other aspects of the underlying communication system. These aspects are associated with the time-varying characteristics of the fading wireless channel, modulation, and the number of antennas in the mobile nodes.

The contributions of our work are in the following areas. We introduce a novel probabilistic connectivity metric for wireless ad-hoc networks relying on an analysis of the time-varying fading wireless channel. Our metric is defined based on the symbol error rate of wireless channels thereby considering the effects of fading and modulation in the mobile nodes.

The rest of this paper is organized as follows. Section II provides an analysis of the received signal-to-interference-noise ratio in time-varying fading Rayleigh channels. We note that our analysis can also be applied to other fading channels such as Rician and Nakagami channels. Section III investigates the problem of connectivity based on a probabilistic treatment of symbol error rates in wireless channels. In Section IV, we numerically validate our connectivity analysis results. Finally, Section V concludes this paper.

II. Analysis of Received Signal-to-Interference-Noise Ratio

In this section, we provide an analysis of the signal-to-interference-noise ratio for a Rayleigh fading channel. We note that a similar analysis can be applied to other fading channels.

Consider q wireless links, labeled $\mathcal{L}_1, \ldots, \mathcal{L}_q$, on which transmission powers are $P_1, \ldots, P_q$, respectively. Link i is associated with the i-th transmitter/receiver pair. The non-negative number $G_{ij}(t)$ represents the path gain in the absence of fading from the transmitter of link j to the receiver of link i at time t. $G_{ij}(t)$ captures such factors as path loss, shadowing, antenna gain, and so on. $F_{ij}(t)$ is the envelope of the fading factor between the transmitter of link j and the receiver of link i. At the end of link i, the power at receiver i is given by

$$G_{ii}(t)P_i(t)F_{ii}(t) \tag{1}$$

Similarly, interfering signals from all of the other links on which P_j's ($i \neq j$) are transmitted are given by

$$G_{ij}(t)P_j(t)F_{ij}(t) \tag{2}$$

The instantaneous signal-to-interference-noise ratio at time t for link i determines the quality of the received signal and is defined as

$$SINR_i(t) = \frac{G_{ii}(t)P_i(t)F_{ii}(t)}{\sum_{j\neq i} G_{ij}(t)P_j(t)F_{ij}(t) + P_i^{(N)}(t)} \tag{3}$$

where $P_i^{(N)}(t)$ represents the power of white Gaussian noise on link i. We assume that the fading factors are Identically and Independently Distributed (IID) when the transmitter and the receiver belong to different links. However, the fading parameters of different links vary depending on the location of the end nodes of the link. Further, the fading factors of each link are temporally correlated. We argue that the latter case represents a channel in which the temporal correlation between $F_{ij}(t)$ and $F_{ij}(t+\triangle t)$ cannot be ignored where $\triangle t$ is a given time shift. In order to capture the temporal correlation of the wireless channel, we make few realistic assumptions as follows. First, the distribution of the white Gaussian noise is independent from the fading distributions. Second, we assume that the fading factors in interfering signals F_{ij}'s with $i \neq j$, are IID, i.e., they are not spatially correlated. Third, when the wireless channel varies slowly with respect to the symbol interval, $P_i(t)$ and $G_{ij}(t)$ can be viewed as constants and $F_{ij}(t)$ as a random variable within the symbol

interval. In the rest of our section, we work with the resulting random variables in the symbol interval.

Based on the above assumptions, we define the average signal-to-interference-noise ratio of link i as

$$\overline{SINR_i} = \frac{E[G_{ii}P_iF_{ii}(t)]}{E[G_{ij}P_jF_{ij}(t)+n_i(t)]} \quad (4)$$

$$= \frac{G_{ii}P_i\overline{F}_{ii}}{\sum_{j\neq i}G_{ij}P_j\overline{F}_{ij}+E_n} \quad (5)$$

where $E[.]$ denotes the expectation operator, $E[F_{ij}(t)] = \overline{F}_{ij}$, and $E[n_i(t)] = E_n$. Given the path gains, transmission powers, statistics of the noise signal, and the first order statistics of of the fading distributions F_{ij}, one can calculate $\overline{SINR_i}$ in the symbol duration from the analysis above.

In our analysis, the output signal of the wireless channel Ω_i and its input S_i in link i can be related as

$$\Omega_i = H_{ii}\,S_i \;+\; \sum_{j\neq i} H_{ij}S_j \;+\; n_i \quad (6)$$

where the fading factors H_{ij} are complex Gaussian random variables and n_i represents the white Gaussian noise. We note that in Equation (6), the undesired effects of interference signals S_j and the noise signal n_i are captured independently. We assume that the receiver of link i knows the channel fading factor H_{ii} while the transmitter of link i only knows its distribution.

It is well established [13] that $r_{ii} = |H_{ii}|$ has a marginal Rayleigh density function when H_{ii} is a complex Gaussian random variable. The density function is expressed as

$$p_R(r_{ii}) = \frac{re^{-r_{ii}^2/2\mu_i^2}}{\mu_i^2}, \;\; r_{ii} \geq 0 \quad (7)$$

where μ_i^2 equals to half of the average power of all of the multipath components.

Since F_{ii} is defined as $F_{ii} = r_{ii}^2 = |H_{ii}|^2$, we are interested in the distribution of $|H_{ii}|^2$. The distribution of $|H_{ii}|^2$ can be calculated by utilizing Equation (7) and the fact that the following equation holds, [13].

$$p_F(F_{ii}) = \frac{1}{2\sqrt{F_{ii}}}p_R(\sqrt{F_{ii}}) \quad (8)$$

We conclude that F_{ii} has a marginal exponential Probability Density Function (PDF) as

$$p_F(F_{ii}) = \frac{e^{-F_{ii}/2\mu_i^2}}{2\mu_i^2}, \;\; F_{ii} \geq 0 \quad (9)$$

A similar argument is applied to the distribution of the random variables F_{ij}.

III. A Probabilistic SER-Based Connectivity Metric

The discussion of this section revolves around providing a probabilistic measure of connectivity based on the characteristics of the underlying communication systems. These characteristics include signal-to-interference-noise ratio, modulation, and symbol error rates.

In [16], expressions of the symbol error rate of a single transmit single receive antenna link in terms of the number of signal points in the constellation L and the average signal-to-noise ratio SNR can be found. As one of the operating scenarios, the calculations are carried out for a Rayleigh fading channel and utilizing the PSK modulation scheme. In what follows, we provide a brief review of the discussion.

First, we pay attention that in the current discussion the quantity of interest is $SINR$ rather than SNR. However, the calculations of [16] are carried out under the assumption of facing a Gaussian noise. Since we are working with $SINR$, we combine the undesired effects of interference and noise signals together. We define

$$N_i \;=\; \sum_{j\neq i} H_{ij}S_j \;+\; n_i \quad (10)$$

As such, Equation (6) is expressed as

$$\Omega_i = H_{ii}\,S_i \;+\; N_i \quad (11)$$

Next, we note that the set of S_j signals in PSK modulation all have the same unit magnitude with a different phase. Consequently, the product $H_{ij}S_j$ remains Gaussian. Since the sum of Gaussian random variables is still Gaussian [13], the noise signal N_i is still Gaussian. However, the resulting Gaussian noise is now colored rather than being white. We note that applying Maximum Likelihood (ML) decoding as utilized by [16] to a colored Gaussian noise results in sub-optimality, i.e., identifying upper bounds of the SER. Nonetheless, the upper bounds are very close to the optimal values of SER. Based on the argument above, the analysis of [16] can still be applied to the case of $SINR$ utilizing the model of Equation (6) the same way it is applied to SNR.

Utilizing the analysis of [16] and given the fading channel characteristic, the symbol error rate of a single transmit single receive antenna link i is introduced as

$$SER_i \;=\; Q\left(\sqrt{\zeta\, F_{ii}\,\overline{SINR_i}}\right) \quad (12)$$

where the Gaussian Q function is defined as

$$Q(x) \;=\; \frac{1}{\sqrt{2\pi}}\int_x^\infty \exp\left(-\frac{z^2}{2}\right) dz \quad (13)$$

In addition, $\overline{SINR_i}$ is the average signal-to-interference-noise ratio at the receive antenna of link i and ζ depends

on the choice of constellation. We note that the discussion of [16] also introduces closed-form expressions for the symbol error rates of a given link under ergodicity assumptions. However, we rely on a probabilistic approach without limiting our discussion to the ergodic case.

It is important to note that SER_i as defined in Equation (12) is a random variable considering the fact that F_{ii} is a random variable. Given the distribution of F_{ii}, the distribution of SER_i can be found by relying on the fundamental theorem of page 130 of [13].

Having calculated the symbol error rate of link i, we can express our metric of connectivity in terms of the quantities of interest. We note that our metric of connectivity is a probabilistic metric. We introduce our probabilistic metric of connectivity as

$$Pr(SER_i > S_{out}) < \Delta_S \tag{14}$$

where $Pr(.)$, S_{out}, and Δ_S represent probability, the threshold of connectivity, and the outage probability, respectively.

We rely on Fig. (1) to explain our metric of connectivity. The figure depicts a normalized sample plot of $1 - CDF(SER)$ where $CDF(SER)$ indicates the Cumulative Distribution Function of SER. For a choice of S_{out} on the horizontal axis, the corresponding value on the vertical axis represents the value $Pr(SER_i > S_{out})$. Thus, the connectivity metric may be satisfied if the horizontal line representing Δ_S is located above the value of $Pr(SER_i > S_{out})$.

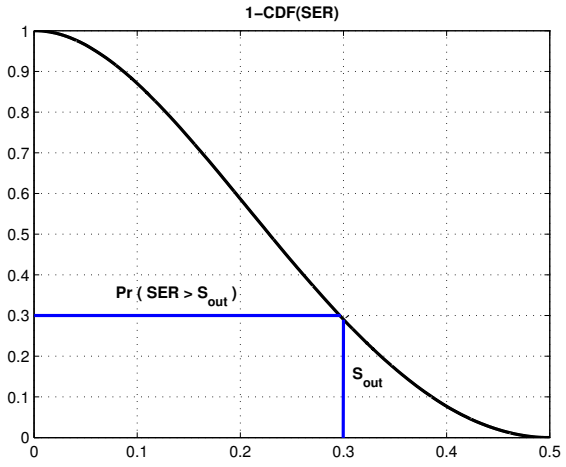

Fig. 1. A normalized sample plot of $1-CDF(SER)$ utilized to illustrate the proposed connectivity metric.

Further, the following example is useful in better understanding the proposed metric of connectivity of (14). In voice communication systems, an error of $S_{out} = 0.001$ is acceptable. That is to say, an outage happens when error rate is more than 0.1% of the conversation. For such a system, our metric implies that if the frequency of outage event in conversations between two nodes is less than Δ_S, we can consider those two nodes connected.

We reiterate that the advantage of using the connectivity metric of this section compared to an $SINR$ metric is that the metric of this section can capture the fading characteristics of the wireless channel as well as the effects of communication system components' in the mobile nodes.

IV. Numerical Validation

We open this section by providing a justification for using our proposed metric of connectivity instead of the $SINR$ metric. Our argument revolves around the fact that the probabilistic measure of the symbol error rate of a link could be different for the same $SINR$ based on the choice of the components of the communication system.

We utilize Fig. 2 to justify our argument. For different choices of L in an L-PSK modulation scheme, Fig. 2 depicts normalized values of $1 - CDF(SER)$ versus S_{out}.

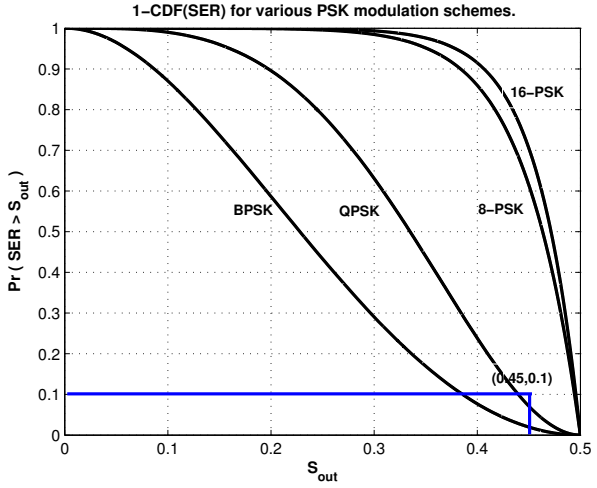

Fig. 2. Normalized sample plots of $1-CDF(SER)$ for different choices of L-PSK.

The figure reveals the fact that the probabilistic measure of the symbol error rate can be different for the same signal strength based on the choice of modulation. For example, for the choice of $(S_{out}, \Delta_S) = (0.45, 0.1)$, the connectivity metric of (14) is satisfied for a wireless link utilizing BPSK or QPSK modulation but not 8-PSK or 16-PSK.

Hence, depending on the thresholds of connectivity S_{out}, and Δ_S that are determined by the hardware and software computing platform of a mobile node, a pure measurement of the signal strength such as $SINR$ is not quite capable of describing connectivity.

Next, we apply our proposed connectivity scheme to a random ad-hoc topology. In order to provide a meaningful basis

of comparison, we compare our results for the same topology. In our random topology, 200 nodes are distributed on a 2-D domain with an area of 1000 square meters according to a Poisson point process.

Before proceeding with the explanation of our results, we note that we are investigating the connectivity of wireless ad-hoc networks accommodating mobile nodes in a wireless fading environment. We assume that the fading wireless channel characterized by a Rayleigh distribution is quasi-static and flat implying that the path gains are constant over a symbol but vary independently from one symbol to another.

The following describes general settings of our experiments. The gains for each link are computed as $G_{ii} = \frac{1}{d_{ii}^3}$ and $G_{ij} = \frac{\eta}{d_{ij}^3}$ for $i \neq j$, where d_{ij} represents propagation path length from the transmitter of link j to the receiver of link i. The factor η can be viewed as the power falloff with frequency in an FDMA system, or the spreading gain in a CDMA system. It is set as $\eta = 0.002$ in our simulations.

We assume that each node utilizes a total transmission power of $P = 1W$ on the combined set of its outgoing links. The expected value of the noise power on each path is assumed to be $10\mu W$. Depending on a specific experiment, a pair of nodes are considered to form a direct link $\mathcal{L}_i$ if the probabilistic connectivity metric of (14) holds. We note that link connectivity may be directional implying that a first node can transmit to a second node while the second node may not be able to transmit to the first node. In our experiments, we consider link connectivity to exist only if both nodes can transmit and receive from each other under our connectivity criterion.

For the random topology described above, we consider four scenarios associated with different choices of L in L-PSK modulation.

The illustrations of Fig. 3 show the connectivity graphs of our connectivity metric for the given random topology network. Reviewing the connectivity graphs, we observe that the connectivity graphs of the topology vary depending on not only the signal-to-interference-noise-ratio but the symbol error rate characteristics. On the contrary to an $SINR$-based metric, utilizing our proposed metric provides a precise way of properly capturing the effects of the quantities of interest when investigating connectivity. Generally speaking, the choice of connectivity metric depends on the characteristics of the underlying wireless channel and the information available about the components of the communication system. From the results of the experiments, we can also calculate the percentages of the nodes belonging to the largest connected cluster of nodes.

Utilizing the connectivity metric of (14), Table I reports the connectivity results for three different combination of choices of S_{out} and Δ_S with similar other settings.

TABLE I

A COMPARISON OF THE RELATIVE SIZES OF THE LARGEST CONNECTED CLUSTER UTILIZING THE PROBABILISTIC SER CONNECTIVITY METRIC OF (14).

	$S_{out} = 0.2$ $\Delta_S = 0.2$	$S_{out} = 0.3$ $\Delta_S = 0.2$	$S_{out} = 0.3$ $\Delta_S = 0.3$
16-PSK	2%	2.5%	4%
8-PSK	7%	10%	15.5%
QPSK	89.5%	94%	94%
BPSK	97%	97%	98%

We observe that increasing the value of S_{out} and Δ_S increases the size of the largest cluster of the connectivity graph. We also observe that increasing the number of points in a constellation decreases the size of the largest cluster of the connectivity graph. The latter is expected as increasing the number of points in a constellation increases the probability of error.

We note that for any given topology, the connectivity of an ad-hoc network depends on the choice of connectivity parameters and the specific topology of the network.

V. CONCLUSION

In this paper, we investigated the connectivity of fading wireless ad-hoc networks. We analyzed the time-varying fading characteristics of signal-to-interference-noise ratio ($SINR$) of the wireless channel. By defining a novel probabilistic metric of connectivity, we investigated the problem of connectivity based on the symbol error rate rather than the received signal strength. Our results clearly captured the effects of communication system components in the connectivity of wireless ad-hoc networks. Our future research is focused on the extension of our results to the case of MIMO wireless channels. Further, we are investigating the applicability of our results in the context of cross-layer routing and scheduling schemes for wireless ad-hoc networks.

REFERENCES

[1] F. Baccelli, B. Blaszczyszyn, "On A Coverage Process Ranging from the Boolean Model to the Poisson Voronoi Tessellation, with Applications to Wireless Communications," Advance Applied Probability, vol. 33(2), 2001.

[2] C. Bettstetter, "On the Minimum Node Degree and Connectivity of a Wireless Multihop Network," In Proc. ACM MOBIHOC, 2002.

[3] L. Booth, J. Bruck, M. Franschetti, R. Meester, "Continuum Percolation and the Geometry of Wireless Networks," Annals of Applied Probability, 2002.

[4] Y.-C. Cheng, T. G. Robertazzi, "Critical Connectivity Phenomena in Multihop Radio Models," IEEE Trans. Communications, July 1989.

[5] O. Dousse, P. Thiran, M. Hasler, "Connectivity in Ad-Hoc and Hybrid Networks," In Proc. IEEE INFOCOM, 2002.

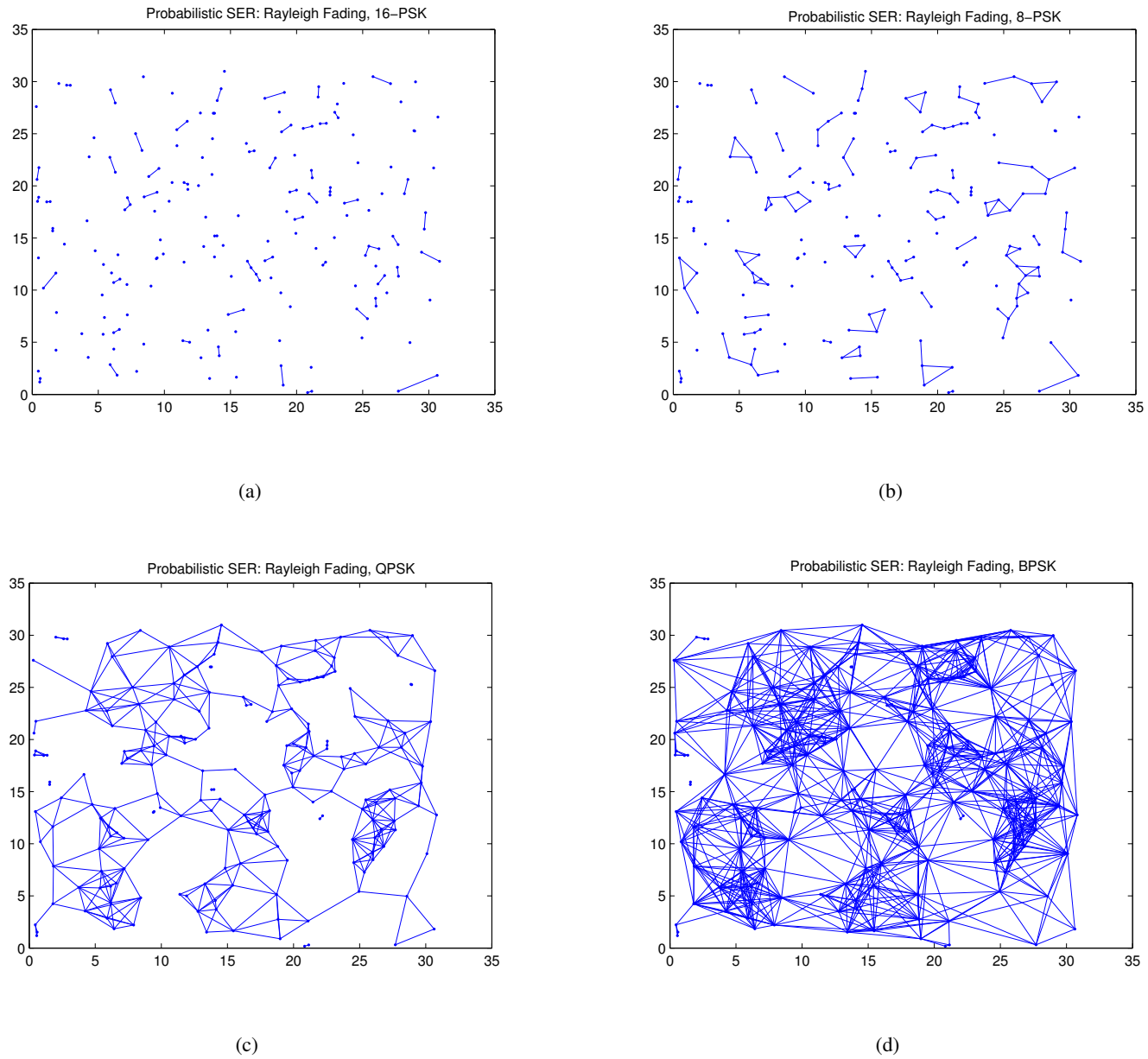

(a) (b)

(c) (d)

Fig. 3. Connectivity graphs of a random topology network in a square domain of 1000 square meters with the same thresholds of connectivity S_{out} and Δ_S. The choices of modulation scheme include (a) 16-PSK, (b) 8-PSK, (c) QPSK, and (d) BPSK.

[6] O. Dousse, F. Baccelli, P. Thiran, "Impact of Interferences on Connectivity in Ad-Hoc and Networks," In Proc. IEEE INFOCOM, 2003.

[7] E. N. Gilbert, "Random Plane Networks," SIAM J., vol. 9, pp. 533543, 1961.

[8] G. Grimmett, "Percolation, 2nd Edition," Springer, ISBN 3540649026, 1999.

[9] M. Grossglauser, D. Tse, "Mobility Increases the Capacity of Ad-Hoc Wireless Networks," In Proc. of IEEE INFOCOM, 2001.

[10] P. Gupta, P. R. Kumar, "Critical Power for Asymptotic Connectivity in Wireless Networks," Stochastic Analysis, Control, Optimization and Applications: A Volume in Honor of W.H. Fleming, 1998, edited by W.M. McEneany, G. Yin, and Q. Zhang, (Eds.) Birkhauser.

[11] P. Gupta, P. R. Kumar, "The Capacity of Wireless Networks," IEEE Trans. Information Theory, March 2000.

[12] R. Meester, R. Roy, "Continuum Percolation," Cambridge University Press, ISBN 052147504, 1996.

[13] A. Papoulis, S.U. Pillai, "Probability, Random Variables, and Stochastic Processes, Fourth Edition," McGraw-Hill, ISBN 0071122567, 2002.

[14] S. Quintanilla, S. Torquato, R.M. Ziff, "Efficient Measurements of the Percolation Threshold for the Fully Penetrable Disks," Journal of Physics, October 2000.

[15] P. Santi, D.M. Blough, "An Evaluation of Connectivity in Mobile Wireless Ad Hoc Networks," In Proc. IEEE DSN, 2002.

[16] M.K. Simon, M.S. Alouini, "Digital Communication over Fading Channels: A Unified Approach to Performance Analysis," John Wiley, ISBN 0471317799, 2000.

[17] D. Watts, S. Strogatz, "Collective Dynamics of Small-World Networks," Nature, June 1998.